

REPORT DOCUMENTATION PAGE

Form Approved
OMB NO. 0704-0188

Public Reporting burden for this collection of information is estimated to average 1 hour per response, including the time for reviewing instructions, searching existing data sources, gathering and maintaining the data needed, and completing and reviewing the collection of information. Send comment regarding this burden estimates or any other aspect of this collection of information, including suggestions for reducing this burden, to Washington Headquarters Services, Directorate for Information Operations and Reports, 1215 Jefferson Davis Highway, Suite 1204, Arlington, VA 22202-4302, and to the Office of Management and Budget, Paperwork Reduction Project (0704-0188), Washington, DC 20503.

1. AGENCY USE ONLY (Leave Blank)		2. REPORT DATE		3. REPORT TYPE AND DATES COVERED Final Report 4/1/98-3/31/01	
4. TITLE AND SUBTITLE Studies of Transport Phenomena and Their Effect on Weld Quality in Laser Beam Welding				5. FUNDING NUMBERS Grant No.DAAG55-98-1-0097	
6. AUTHOR(S) Dr. Hai-Lung Tsai					
7. PERFORMING ORGANIZATION NAME(S) AND ADDRESS(ES) University of Missouri-Rolla 1870 Miner Circle, Rolla, MO 65409				8. PERFORMING ORGANIZATION REPORT NUMBER	
9. SPONSORING / MONITORING AGENCY NAME(S) AND ADDRESS(ES) U. S. Army Research Office P.O. Box 12211 Research Triangle Park, NC 27709-2211				10. SPONSORING / MONITORING AGENCY REPORT NUMBER 37833-MS	
11. SUPPLEMENTARY NOTES The views, opinions and/or findings contained in this report are those of the author(s) and should not be construed as an official Department of the Army position, policy or decision, unless so designated by other documentation.					
12 a. DISTRIBUTION / AVAILABILITY STATEMENT Approved for public release; distribution unlimited.				12 b. DISTRIBUTION CODE	
13. ABSTRACT (Maximum 200 words) The objective of the project is to study the complicated transport phenomena (laser-material interaction, heat transfer, and melt flow) and their effect on weld quality in laser beam welding. In particular, we are interested in investigating the formation of "keyholes", keyhole dynamics, and possible weld defects caused by keyhole instability. A mathematical model based on continuum formulation (for handling metal flow during alloy melting/solidification) and volume-of-fluid (for handling free surfaces) has been successfully developed to simulate the transient behavior of a keyhole in laser beam welding. We are able to predict, for the first time, 1) the formation and collapse of a keyhole; 2) the formation of porosity in the weld; 3) laser welding with filler metals; 4) laser welding of galvanized steel; and 5) 3-D moving laser welding. Based on the mathematical modeling, we proposed three methods to eliminate/reduce porosity in the weld. Although a direct comparison with experimental results is unavailable, the predicted porosity formation compares favorably with published experimental reports.					
14. SUBJECT TERMS				15. NUMBER OF PAGES	
				16. PRICE CODE	
17. SECURITY CLASSIFICATION OR REPORT UNCLASSIFIED	18. SECURITY CLASSIFICATION ON THIS PAGE UNCLASSIFIED	19. SECURITY CLASSIFICATION OF ABSTRACT UNCLASSIFIED	20. LIMITATION OF ABSTRACT UL		

NSN 7540-01-280-5500

Standard Form 298 (Rev.2-89)
Prescribed by ANSI Std. Z39-18
298-102

20030605 175

Studies of Transport Phenomena and Their Effect on Weld Quality in Laser Beam Welding

Final Progress Report

Grant No. DAAG55-98-1-0097

Submitted to

U.S. Army Research Office

by

Hai-Lung Tsai

Department of Mechanical and Aerospace Engineering and Engineering Mechanics

University of Missouri-Rolla

TABLE OF CONTENTS

	Page
I. Foreword	3
II. Statement of the Problem Studied	4
III. Summary of the Most Significant Results.....	6
1. The Formation of a Keyhole in Laser Welding.....	6
2. The Phenomena of Keyhole Collapse	9
3. The Formation of Pores in the Weld	11
4. Methods to Produce Quality Welds without Pores	14
5. Laser Welding with Filler Metals	17
6. Laser Welding of Galvanized Steel.....	18
7. 3-D Moving Laser Welding	19
IV. List of Publications and Technical Presentations.....	21
V. List of Participating Scientific Personnel.....	22
VI. Technology Transfer to Industry	23
VII. Report of Inventions.....	24

I. Foreword

Scientific knowledge of the transport phenomena and their effects on weld quality is the key to the optimizations of the operation windows in laser beam welding. This project studies the detailed transport phenomena (laser-plasma interactions, laser-material interactions, and molten metal fluid dynamics) and their effects on weld qualities. A comprehensive mathematical model with continuum formulation (for handling metal flow during alloy melting/solidification) and volume-of-fluid (for handling free surfaces) is successfully developed to simulate the transient behavior of a keyhole in laser beam welding. The Fresnel absorption due to multiple laser reflections and the inverse Bremsstrahlung absorption of the laser-induced plasma in the keyhole are taken into account in the models. The following cases are investigated in this project: 1) the formation and collapse of an axisymmetric keyhole 2) formation of porosity and control strategies 3) interaction between filler metals and weld pool 4) zinc vapor escape in laser welding of galvanized steel 5) 3-D moving laser welding.

The simulation predictions are qualitatively consistent with the reported experimental results. Simulation results show that the formation of porosity is caused by two competing mechanisms: one is the solidification rate of the molten metal surrounding the keyhole and the other is the speed at which molten metal backfills the keyhole after laser energy is terminated. By controlling laser pulses or by applying an electromagnetic force after laser energy is ceased, pores in the weld can be reduced or eliminated. The results from simulation illustrate that uniform composition of weld pool is difficult to achieve by filler metals due to very rapid solidification of weld pool in laser welding as compared to that in gas metal arc welding. In laser welding of galvanized steel, by controlling welding parameters, keyhole can be utilized as the channel for releasing the zinc vapor and as a result, pores caused by the trapped zinc vapor are avoided. Avoiding the interaction between zinc vapor and welding pool can improve welding shape. The results from 3D model of laser welding have a very promising potential for industry applications.

II. Statement of the Problem Studied

As laser welding involves very bright, high energy-density laser beam, plasma arc, high temperature, and high welding speed, our current facilities are insufficient for direct observation of the formation and collapse of a keyhole. Alternatively, this project studies the final shape and the final depth of a keyhole under various welding conditions. To our best knowledge, current laser welding technologies are all based on experiences and trial-and-error method. Scientific research is highly desirable for the dramatic promotions of laser technologies in industry.

A mathematical model is developed based on continuum formulation (for handling metal flow during alloy melting/solidification) and volume-of-fluid (for handling free surfaces) to study the transient behaviors of a keyhole in laser beam welding. The model consists of two sub-models: one calculates the mass, momentum and energy transport in the weld pool, and the other determines temperature field of plasma in the keyhole. These two sub-models provide boundary conditions for each other.

For the first time, the formation and collapse of a keyhole and the fluid flow surrounding the keyhole in laser welding becomes predictable using our models. Our investigations reveal that plasma generation in the keyhole decreases penetration depth and increases liquid layer surrounding the keyhole because of radiation of high temperature plasma. As thickness of the liquid layer surrounding the keyhole increases, hydrodynamic force may trigger keyhole collapse.

The second issue of this investigation is porosity in laser welding. Porosity deteriorates the strength of the welded part. This is extremely important in a deeply penetrated laser weld. All previously reported research on porosity formation and prevention are based on experiments and a trial-and-error procedure. This project investigates formation mechanisms of the pore in the laser welding process and the influence of keyhole aspect ratio on pore size via mathematical simulations.

Laser welding with filler metals is the third focus of the project. Recently, laser welding with filler metals has increasingly attracted attention to improve welding quality. Again, all reported studies on laser welding with filler metals are by experiments. Results from the previous investigations demonstrate a general idea of how laser welding can benefit from filler metals, yet the researches fail to reveal the interaction between filler metals and weld pool. Numerical simulations are required to understand the physical phenomena in the welding process. Complicated velocity and temperature fields during the impingement of filler droplets onto the keyhole are simulated in this project. The mixing between base metal and filler metal in the fusion zone is traced by the concentration of sulfur, which is enhanced by the vortex created by the downward momentum along with the impinging droplets. By analyzing the interaction between filler droplets and weld pool, effect of key process parameters on the distribution of filler metals in the final weld bead is investigated.

The fourth issue addressed in this project is laser welding of galvanized steel. Zinc-coated steel is widely used in industry due to its low cost and high corrosion resistance. However, the low melting and evaporation points of zinc tend to produce spatters or porosity in laser lap welding. Most of previous researches on this topic are limited to experimental works. This project examines laser welding of galvanized steel by mathematical simulations. Special attention is paid to zinc vapor formation and zinc escape through the keyhole. Defect control strategies are also discussed.

The latest effort of this project is focused on 3D modeling of laser beam welding. The 3D model is able to uncover the relationship between the laser power and keyhole depth and width by fully analyzing the welding pool dynamics, the temperature field distribution, and plasma characteristics to obtain a better understanding of the pore formation mechanisms. The time-dependent distributions of melt flow velocities and temperatures in the weld pool are

investigated. Parametric studies are conducted to determine key parameters influencing weld pool dynamics and weld penetration.

III. Summary of the Most Important Results

1. The Formation of a Keyhole in Laser Welding

Fig. 1 shows a sequence of the shape of the keyhole during the keyhole formation process. The corresponding temperature and velocity fields are given in Fig. 2 and Fig. 3 respectively. During the initial stage ($t < 1.5$ ms), the laser energy mainly contributes to heating up the base metal. As the temperature of the base metal increases, a weld pool starts to appear under the laser beam, even though it is relatively small and shallow. When the laser power reaches 2500 W, the laser intensity becomes high enough to induce significant recoil pressure. The recoil pressure starts to push down the molten metal under the laser beam. The fluid flow in the weld pool is insignificant at the initial stage. The surface of the weld pool is nearly flat along the top of the substrate. The temperature difference along the free surface of the weld pool is large because of the Gaussian distribution of the laser power, leading to a high temperature-dependent Marangoni shear.

As shown in Fig. 1, although the liquid-solid interface keeps moving downwards, the liquid region of the weld pool under laser radiation remains a thin layer because the strong recoil pressure squeezes the liquid metal to flow outward. As the surface level moves down and the crater level increases, a keyhole is formed in the weld pool. After formation of the keyhole, some metal vapors are trapped in the hole. During the laser penetration process, the gas is heated up very quickly because the low heat capacity of gas. When the temperature of the gas exceeds about 8000 K, laser-induced plasma is generated by ionization. The coefficient of the inverse-Bremsstrahlung absorption increases with the increase of plasma temperature. So once plasma grows, the temperature will increase very quickly, as shown in Fig. 3. Meanwhile, the travel

distance of laser light increases with the development of the keyhole. The absorption of laser power by the gas decreases the radiation intensity. At the same time, plasma separates the keyhole wall from the cold shielding gas. The hot plasma heats the surrounding keyhole wall through heat radiation. This increases the temperature on the keyhole wall. As shown in Fig. 2, the temperature on the keyhole wall keeps increasing, which leads to the increase of recoil pressure.

The formation of the keyhole enhances the laser light absorption through a mechanism called multiple reflections. As shown in Fig. 1, the surface of the weld pool is nearly flat at the beginning. Once laser light radiates the flat surface, only part of the energy is absorbed by the surface through the Fresnel absorption mechanism. A large amount of laser energy is reflected. However, when the keyhole is formed, the surface along the keyhole wall is not flat. The reflected laser light by this surface is not always in the reverse direction of incidence. During each incidence onto the keyhole wall, a fraction of laser energy is absorbed by the Fresnel absorption mechanism. This brings more laser energy to the keyhole wall. Moreover, as the keyhole deepens, the possibilities and times of multiple reflections increase. When the reflected laser light travels in the plasma, part of its energy is absorbed by the plasma, which increases the temperature of plasma. Consequently, the higher temperature of plasma increases the recoil pressure. The influence of the plasma and multiple reflections are shown in Fig. 1. On the bottom surface of the keyhole, higher recoil pressure leaves a thinner liquid layer at $t = 8.5$ ms compared with that at $t = 5.0$ ms. Even though the hydrostatic pressure and surface tension at the bottom of the keyhole becomes larger as the keyhole deepens, which makes it difficult for the drilling process of the keyhole, the velocity of liquid along the bottom surface does not decrease, as shown in Fig. 3.

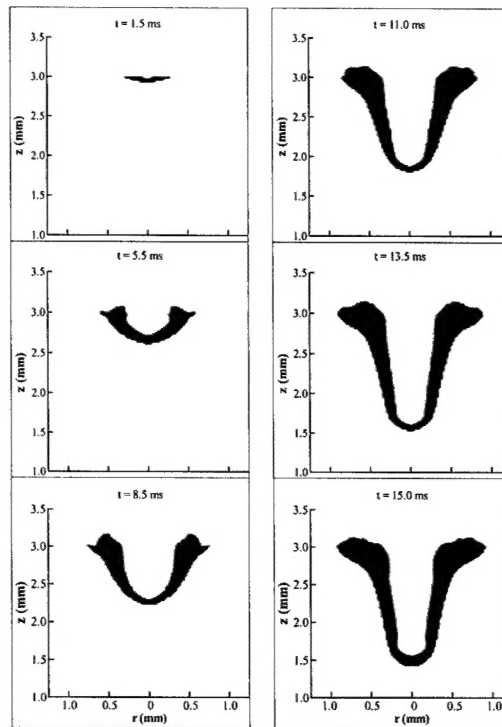


Fig. 1. A sequence of the keyhole formation process showing the shape of the keyhole and the solidification process.

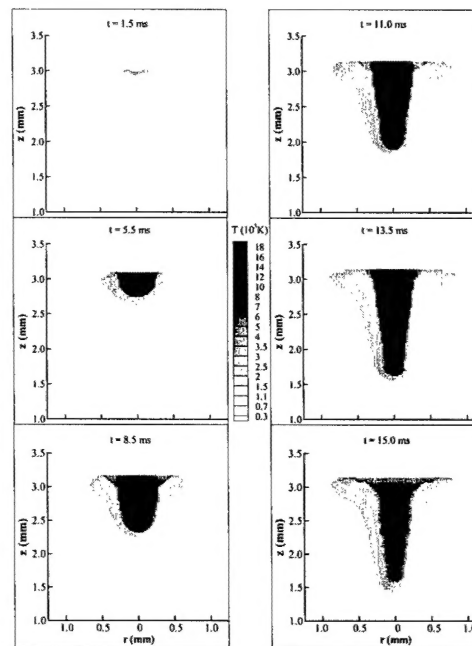


Fig. 2. The corresponding temperature profiles for the case as shown in Fig. 1.

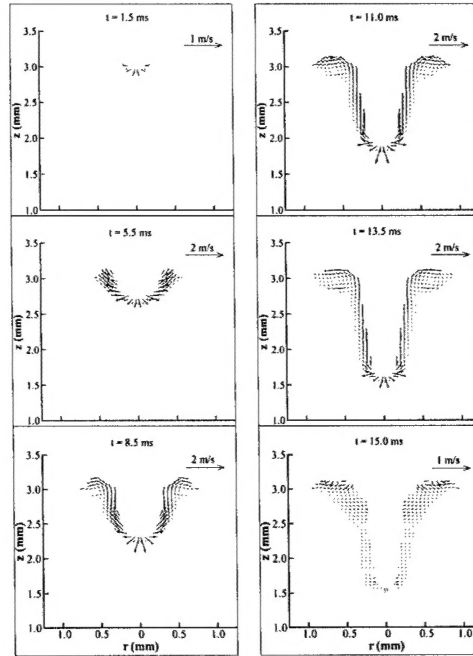


Fig. 3. The corresponding velocity distributions for the case as shown in Fig. 1.

2. The Phenomena of Keyhole Collapse

When the laser pulse is shut off, the recoil pressure is removed correspondingly. The keyhole collapses under hydrostatic pressure and surface tension. Fig. 4 shows a sequence of liquid metal region evolution during the process of keyhole collapse. The corresponding temperature and velocity profiles are given in Fig. 5 and Fig. 6. At $t = 15.0$ ms and $t = 16.5$ ms, the plasma temperature in Fig. 5 drops very quickly, compared with that in Fig. 2. The heat input from plasma radiation also decreases very quickly in a short time. Meanwhile, the heat conduction from the keyhole wall to the surrounding metal is very strong because of high aspect ratio and high temperature gradient. So the temperature of the keyhole wall drops off very quickly, especially in the lower part of the keyhole because there is only a thin layer of metal liquid. Simulations show that the keyhole will close on the top at first and then fill back to the keyhole in the collapse process. Some gas will be trapped during the collapse process. The liquid metal on the far end of the top surface cannot flow back before solidification, which results in a rough surface on the final weld.

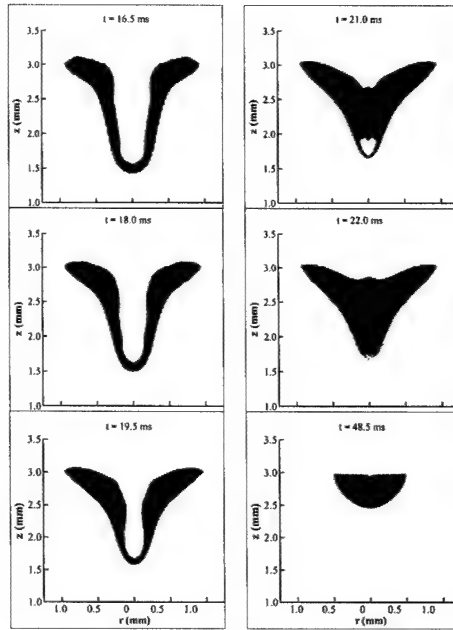


Fig. 4. A sequence of liquid metal region evolution during keyhole collapse process.

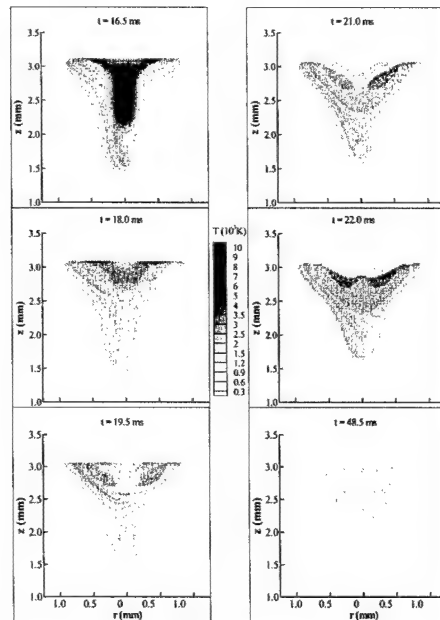


Fig. 5. A sequence of temperature field evolution during keyhole collapse process.

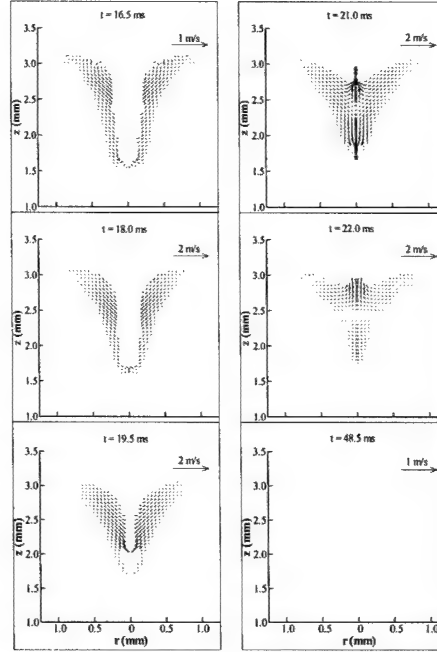


Fig. 6. A sequence of velocity field evolution during keyhole collapse process.

3. The Formation of Pores in the Weld

Fig. 7 shows the evolution of molten metal region during pore formation process. The corresponding temperature and velocity distributions are given in Fig. 8 and Fig. 9 respectively. As the plasma gas has a very small thermal capacity, right after the laser power is ceased, the plasma temperature decreases rapidly. As shown in Fig. 7 for $t = 15.0$ ms, during the keyhole formation process, a large amount of metal liquid is squeezed onto the shoulder of the keyhole under the action of laser induced recoil pressure and surface tension. There is a vortex on the keyhole shoulder as shown in Fig 9 at $t = 15.0$ ms, which enhances the heat transfer from the liquid metal to the substrate. So the liquid metal layer on the upper keyhole is thicker than that on the lower keyhole. When the laser pulse is shut off, the energy input to the keyhole wall comes only from the hot plasma radiation. However, since there is no heat input to the plasma and the heat capacity of plasma is very small, the temperature of plasma drops off very quickly. The heat input from plasma radiation also decreases very quickly in a short time. Meanwhile, the heat conduction from the keyhole wall to the surrounding metal is very strong because of high

aspect ratio and high temperature gradient. So the temperature of the keyhole wall drops off very quickly, especially in the lower part of the keyhole because there is only a thin layer of liquid metal. As shown in Fig. 8, the temperature on the keyhole wall drops off very quickly from $t = 15.0$ ms to $t = 19.2$ ms, especially at the bottom of the keyhole. The study reveals that a pore is formed during the process of the keyhole collapse. The formation process has a close relationship with two factors: one is backfill time, and the other is backfill speed. If the backfill speed of the liquid on the upper of the keyhole is not high enough to completely fill back the keyhole before the liquid metal is solidified, pore forms in the final weld. Aspect ratio of the keyhole has a great influence on pore formation: the larger the aspect ratio, the larger the pore size. When aspect ratio is smaller than threshold value, no pore is observed.

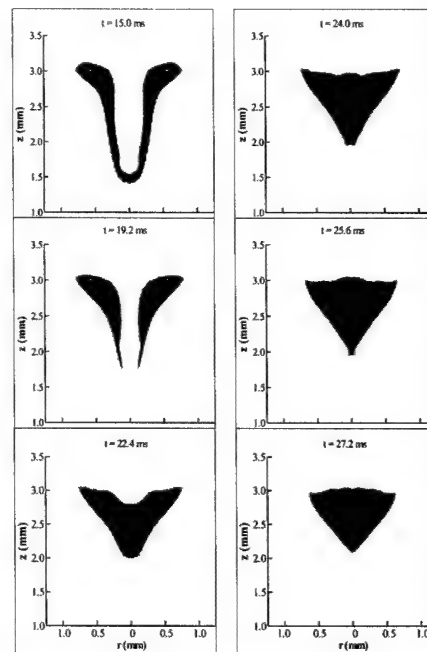


Fig. 7. A sequence of liquid metal region evolution during the pore formation process.

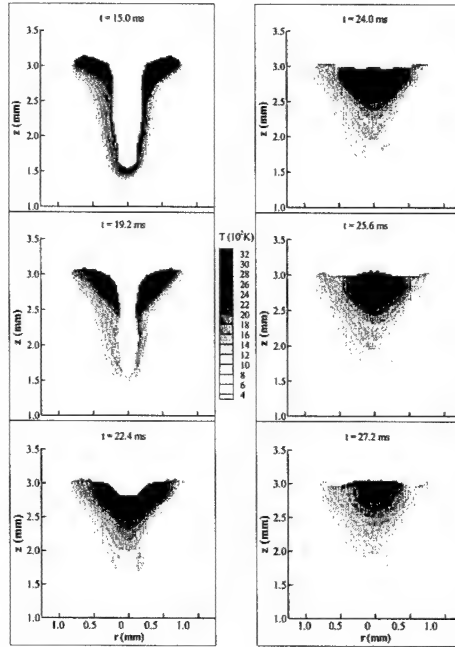


Fig. 8. A sequence of temperature field evolution during pore formation process.

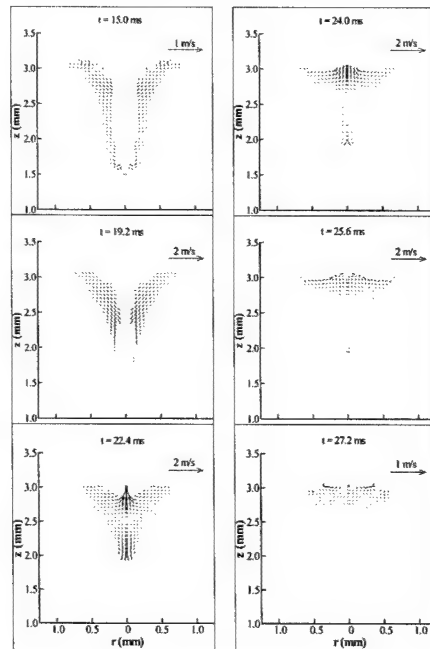


Fig. 9. A sequence of velocity field evolution during pore formation process.

4. Methods to Produce Quality Welds Without Pores

Our simulations show that the method of pulse control can be employed to prevent pores if aspect ratio keyhole is small. Pulse control increases the backfill time to allow the liquid metal on the upper portion of the keyhole to have enough time to flow down. If the aspect ratio is high, the method of electromagnetic force should be applied. The mechanism of exerting an electromagnetic field is to increase the backfill speed, which allows the liquid metal on the upper part of the keyhole to reach the keyhole bottom during backfill time. An electromagnetic field is added once the laser pulse is shut off. The laser power is decreased to one-fifth its peak value and lasts for another 5 ms. The sequence of liquid metal evolution during the keyhole collapse with process electromagnetic force is shown in Fig. 10. The corresponding sequence of liquid metal region evolution and velocity field during the pore formation process is shown in Fig. 11 and Fig. 12. At $t = 15.0$ ms, the laser power is shut off, which removes the recoil pressure and lets the liquid metal in the keyhole to flow back under the gravity and surface tension.

The electromagnetic force that is added shortens the time for the fluid to change its velocity direction. As shown in Fig. 12, the velocity direction of the liquid changes more quickly than that in Fig. 9. As shown in Fig. 12, the electromagnetic force also shortens the time for the keyhole to collapse. Comparing the figure at $t = 19.8$ ms in Fig. 12 with that in Fig. 9, the keyhole is closed far ahead under the electromagnetic force. Similar to what is shown in Fig. 9, the liquid-solid interface moves inward since there is no heat input to the keyhole wall after the laser is shut off at $t = 15.0$ ms, especially on the bottom of the keyhole because the liquid zone is much thinner than that on the shoulder. Because the liquid in the mush zone and near the liquid-solid interface bears larger friction to move, the effect of electromagnetic force on this part of liquid is not as remarkable as that on the shoulder of the keyhole. So the addition of the electromagnetic force has no big influence on the solidification process on the bottom of keyhole. There is no liquid metal left on the bottom. Although the high heat loss also makes the

temperature on the wall drop off and the liquid-solid interface approaches the center quickly, the high downward velocity allows the liquid enough time to reach the bottom of the keyhole, as shown at $t = 20.4$ ms. Since the upper part of void is surrounded by the liquid, the trapped gas is dissolved into the liquid. At the $t = 22.8$ ms, there is no pore left in the keyhole.

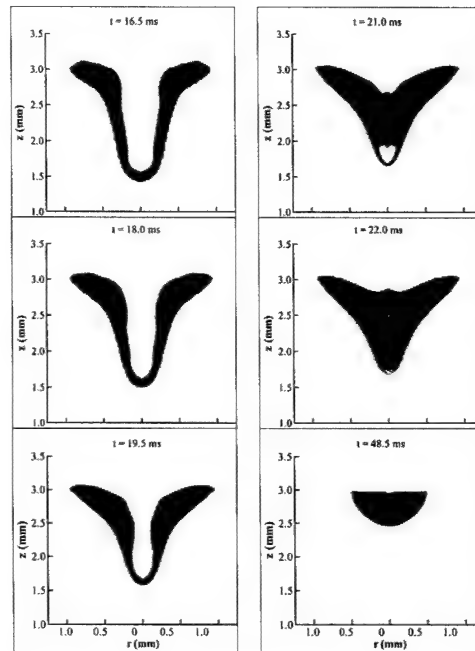


Fig. 10. A sequence of keyhole collapse process showing the shape of the keyhole and the solidification process.

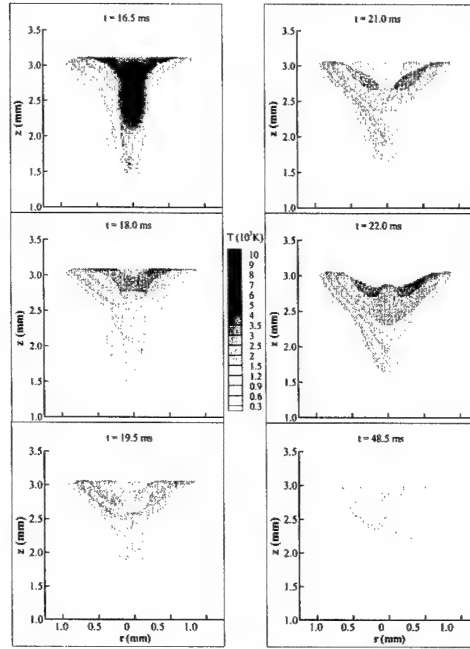


Fig. 11. The corresponding temperature profiles for the case as shown in Fig. 10.

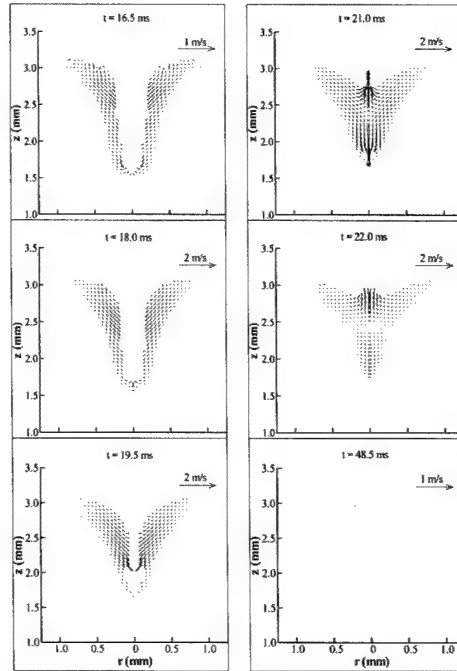


Fig. 12. The corresponding velocity distributions for the case as shown in Fig. 10.

5. Laser Welding with Filler Metals

As shown in Fig. 13, with the increase of droplet diameter, the latitude diffusion of filler metal is enlarged. The above analysis of welding process shows the latitude diffusion of filler metal is closely related with the vortex in the weld pool. The strength and the affected zone of the vortex depends on the downward momentum carried by droplets, which is the product of droplet mass and velocity. As the droplet size increases, the downward momentum increases, which will lead to a stronger vortex. So the diffusion zone is enlarged outwards, especially in the middle depth of the keyhole where the vortex is located. This can be proven by comparing the figures of $d = 0.30$ mm with that of $d = 0.35$ mm in Fig. 13. Meanwhile, a larger downward momentum from larger droplets also leads to strong bouncing flow near the center of keyhole after termination of droplet feeding, which helps filler metal to diffuse into the upper layer in the final weld, as shown in Fig. 13 for $d = 0.40$ mm. After the termination of droplet feeding, the fluid surface near the center of the keyhole continues to go down due to the larger hydrodynamic pressure caused by the downward momentum. This leads to a deep hole. During the back-filling process of this hole, some metal from the upper portion of the keyhole may flow into the bottom of this hole. Since the concentration of filler metal in the upper portion of the keyhole is very low, it will leave a low diffusion zone of filler in the center of final weld, as shown in Fig. 13 for $d = 0.40$ mm. Our simulations on this topic show that filler metals can effectively control pore formation, better welding pool, and improve weld bead shape.

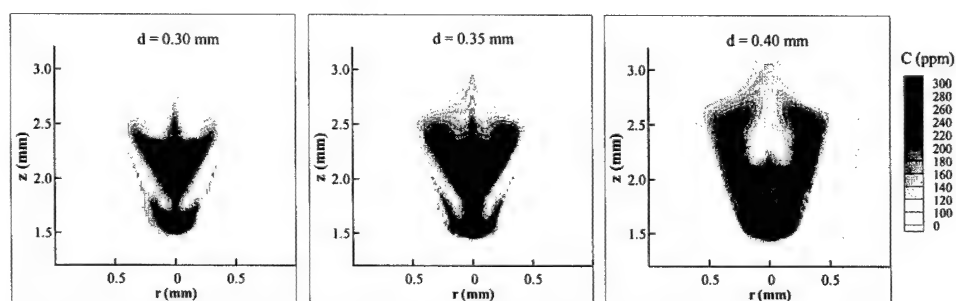


Fig. 13. Effect of droplet size on the diffusion of filler in the fusion zone.

6. Laser Welding of Galvanized Steels

The simulations of laser welding of galvanized steel show the zinc coating is melted and vaporized when the temperature reaches its vaporization point. Because there is no way for the zinc vapor to escape, the zinc vapor is trapped and accumulates to a very high pressure. When the welding reaches a certain depth, the accumulated vapors burst out and interact with the welding pool, which may cause pore formation and spatter. Fig. 14 shows the process of the zinc vapor escape and its interaction with the welding pool. By controlling the laser processing parameters such as laser power and welding speed, keyhole can be utilized as an effective channel for the zinc vapor to escape and thereby the pore formation and spatter are avoided.

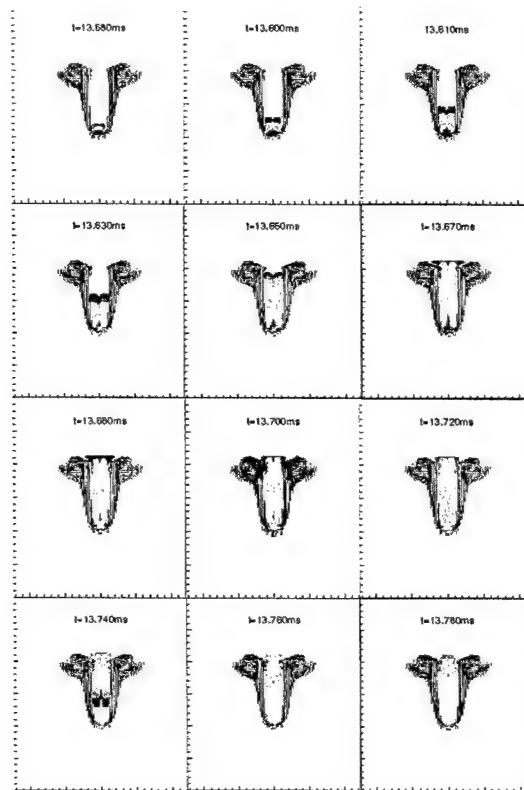


Fig. 14. Keyhole formation & zinc vapor escape during laser welding of galvanized steel.

7. 3-D Moving Laser Welding

3D simulations show that for given welding conditions, there is a relationship between laser power, welding depth and welding width. In the results shown below, the base metal is assumed to be 304 stainless steel containing 100 ppm of sulfur. The laser power is 4.0 KW, the radius at focus spot is 0.2mm, the laser scanning speed is 25mm/s, and laser beam obeys Gaussian distribution. Fig. 15 shows the keyhole depth and width from X-Z plan and Y-Z plan views at different time points. Fig. 16 shows the welding pool shapes from X-Z plan and Y-Z plan views in different time points. Fig. 17 shows the corresponding temperature distribution of both welding pool and plasma inside the keyhole. Fig. 18 shows the corresponding velocity fields in the welding pool.

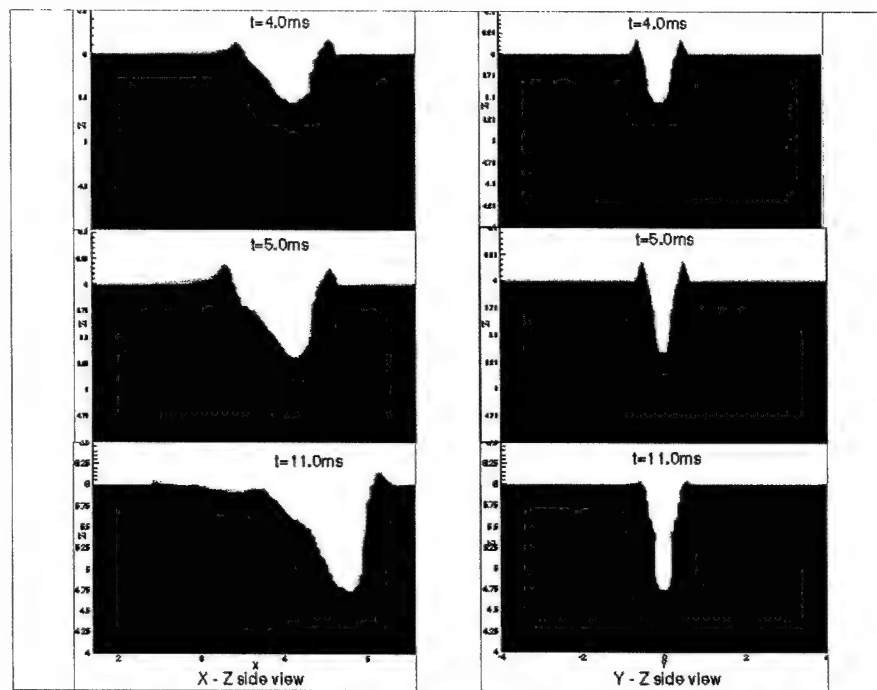


Fig. 15. X-Z plan and Y-Z plan views of the keyhole depth and width.

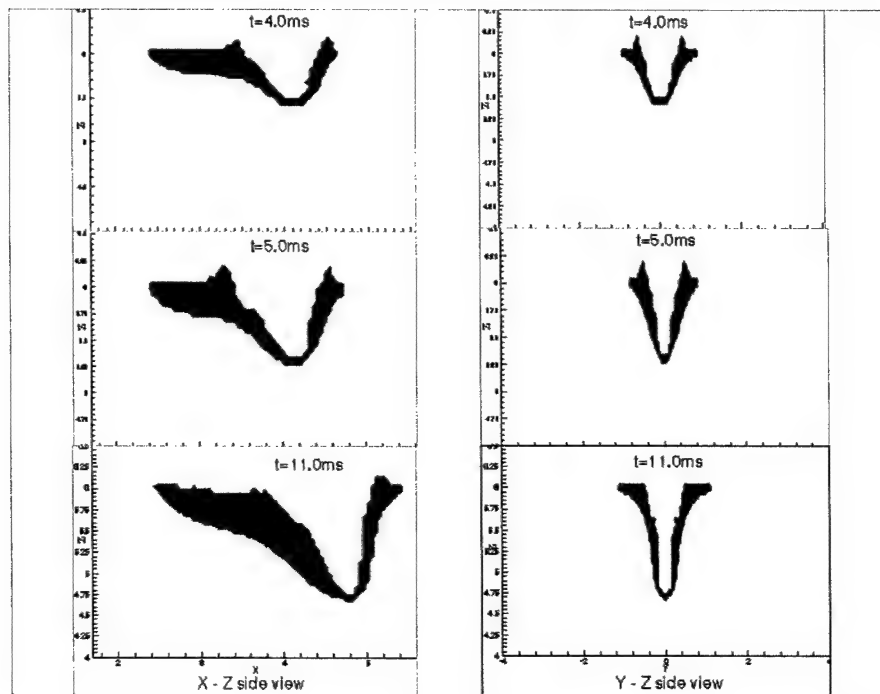


Fig. 16. X-Z plan and Y-Z plan views of the weld pool shapes.

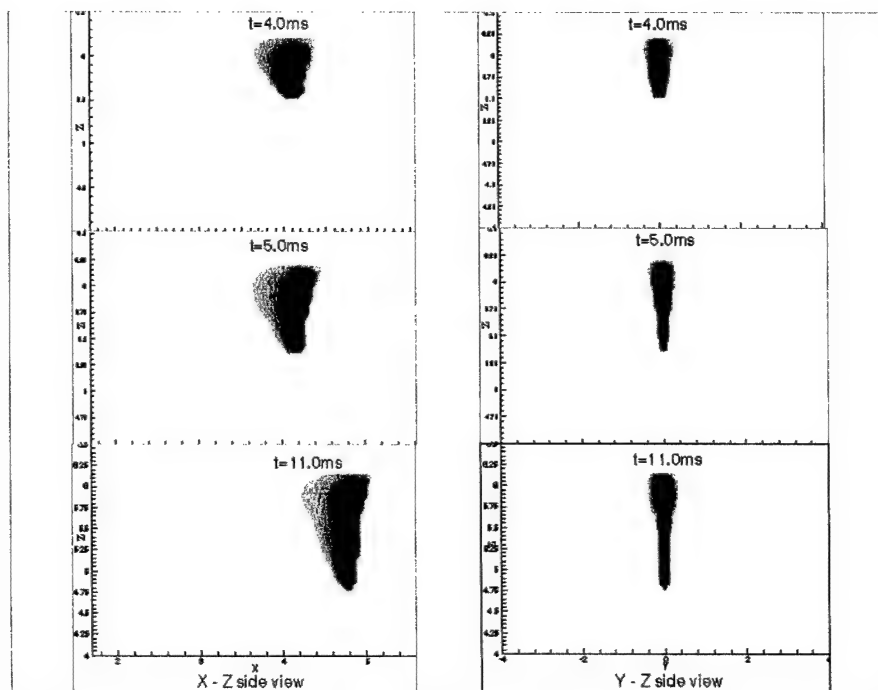


Fig. 17. Temperature distribution corresponding to Figs. 15 and 16.

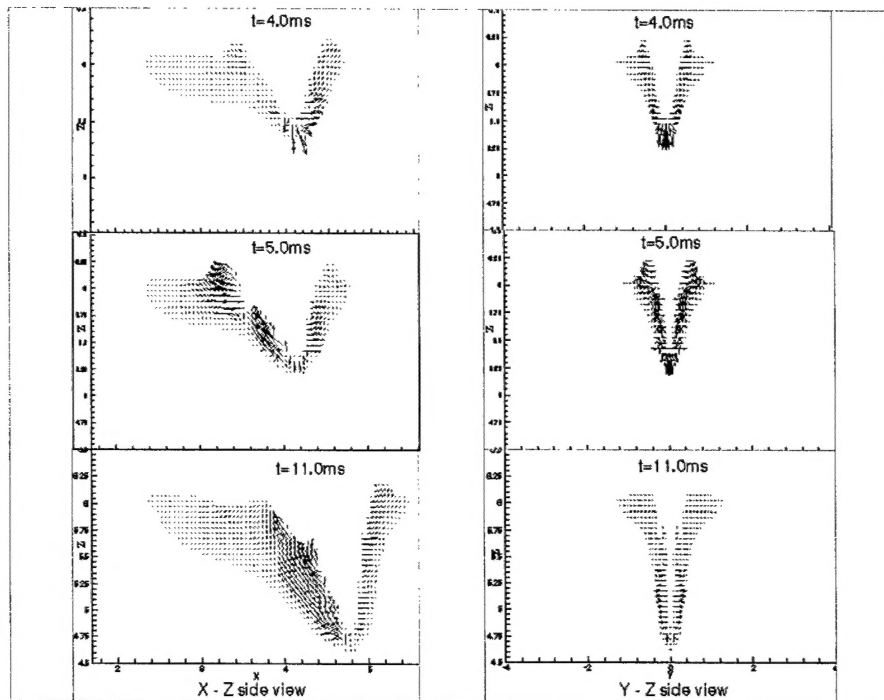


Fig. 18. Velocity fields corresponding to Figs. 19 and 20.

IV. List of Publications and Technical Presentations

Publications:

1. H. G. Fan, H. L. Tsai, and S. J. Na, "Heat Transfer and Fluid Flow in a Partially or Fully Penetrated Weld Pool in Gas Tungsten Arc Welding," *Int. J. Heat Mass Transfer*, 2001, vol. 44, 417-428.
2. H. G. Fan and H. L. Tsai, "A Unified Model for GTA Welding, Including Cathode, Arc Plasma, and Molten Pool" (to be submitted to *Metallurgical and Materials Transactions*).
3. Y. Wang and H. L. Tsai, "Impingement of Filler Droplets and Weld Pool Dynamics in Gas Metal Arc Welding," *Int. J. Heat Mass Transfer*, 2001, vol. 44, pp. 2067-2080.
4. Y. Wang and H. L. Tsai, "Effects of Surface Active Elements on Weld Pool Flow in Gas Metal Arc Welding," *Metallurgical and Materials Transactions B*, 2001, vol. 32B, pp. 501-515.
5. W.H. Zhang, Modeling the formation and Collapse of a Keyhole during Laser Welding Process, Ph.D. Thesis, University of Missouri-Rolla, 2002.

6. W. H. Zhang and H. L. Tsai, "Modeling the Formation and Collapse of a Keyhole during Pulsed Laser Welding Process" (to be submitted).
7. W. H. Zhang and H. L. Tsai, "Modeling the Porosity Formation during Laser Welding Process"(to be submitted).
8. W. H. Zhang and H. L. Tsai, "Modeling the Laser Welding Process with Filler Metals" (to be submitted).
9. W. H. Zhang and H.L. Tsai, "Pore Formation and Prevention in Deep Penetration Pulsed Laser Welding," to be presented in ICALEO 2002, Scottsdale, Arizona, October 14-17, 2002.
10. W. Zhang, J. Zhou, and H.L. Tsai, "Numerical Simulations of Keyhole Dynamics in Laser Welding," to be presented in Osaka, Japan, LAMP 2002, May 27 – 31, 2002.

Technical Presentations:

1. "Modeling of Weld Pool Dynamics in Gas Metal Arc Welding Process," Caterpillar Inc., Peoria, IL, August 12, 1999.
- 2 "Modeling of Gas Metal Arc Welding Process," Caterpillar Inc., Peoria, IL, March 31, 2000.
- 3 "Modeling of Gas Metal Arc Welding Process," Lincoln Electric Company, Cleveland, Ohio, September 21, 2000.
- 4 "Modeling Fluid Flow and Keyhole Dynamics in Laser Welding," GM R&D Center, Warren, MI, March 5, 2001.
- 5 "Basic and Applied Research in Gas Metal Arc Welding at UMR," Department of Materials Science & Engineering, National Cheng-Kung University, Taiwan, May 31, 2001.
- 6 "Basic and Applied Research in Laser Beam Welding at UMR," Department of Naval Architecture and Marine Engineering, National Cheng-Kung University, Taiwan, June 1, 2001.
- 7 "Modeling of Laser Beam Welding Process," GM R&D Center, Warren, MI, December 3, 2001.

V. List of Participating Scientific Personnel

1. Dr. Hai-Lung Tsai, Professor, PI of the project.
First recipient of the newly established "Faculty Research Excellence Award," Academy of Mechanical Engineers, UMR, 9/30/1999.
2. Mr. Yun Wang, received a Ph.D. degree in August 1999.

3. Mr. Wenhai Zhang, Ph.D., defended dissertation in February 2002.
4. Mr. Jun Zhou, Ph.D. candidate.
5. Mr. James A. Barnett, as part of the OURE (Opportunity for Undergraduate Research Experience) program at UMR.
6. Mr. Thomas M. Simon, as part of the OURE program at UMR. Tom's final project report and presentation, entitled "Laser Welding of Aluminum Alloys," received a second place in the OURE competition.

VI. Technology Transfer to Industry

During the project period, we have presented technical seminars and interacted with the following companies or institutions for technical exchange:

1. GM R&D Center, Warren, Michigan.
2. GM Midsize & Luxury Car Group, Warren, Michigan.
3. Caterpillar Technical Center, Peoria, Illinois.
4. System & Electronics Inc., West Plains, Missouri (this is an Army contractor building tank carriers).
5. Missouri Enterprise, Rolla, Missouri.
6. TRW Vehicle Safety Systems, Washington, Michigan.
7. Watlow Heater Technology Center, Fenton, Missouri.
8. Hydro Raufoss Automotive, Holland, Michigan.
9. Department of Mechanical Engineering, University of Michigan, Ann Arbor, Michigan.

Also, several research contracts related to this project have been received during the research period, and they are listed below:

- 1) "Modeling of Gas Metal Arc Welding Weld Pool in the Low Current Regime – 2nd Year," GM R&D Center, \$106,190, 4/1/99-3/31/00.
- 2) "Development of Welding Performance Data for MIG Aluminum Welding," GM Midsize and Luxury Car Group, \$130,500, 7/1/99-12/31/00.
- 3) "Modeling of Transport Phenomena in Gas Metal Arc Welding of Aluminum Alloys," GM R&D Center, \$97,000, 5/00-4/01.
- 4) "Integration and Validation of Gas Metal Arc Welding Models," GM R&D Center, \$117,000, 5/01-4/02.

- 5) "Acquisition of a Friction Stir Welding Equipment for Metal Joining Research and Education," NSF/UMR, \$189,750, 6/00-5/01. (PI: R. Mishra, Co-PIs: H. L. Tsai, D. C. Van Aken)
- 6) "Acquisition of a High-Power Laser System for Research and Education in Manufacturing and Materials Processing," NSF/UMR/UM Research Board, \$487,000, 9/01-2/03. (PI: H. L. Tsai, Co-PIs: J. Choi, R. Landers, M. Leu, M. Rahaman, A. Midha, J. Story, D. C. Van Aken)
- 7) "Integration and Validation of Gas Metal Arc Welding Models," GM R&D Center, \$117,000, 5/01-4/02. (PI: H. L. Tsai)
- 8) "Mathematical Modeling and Experimental Validation of Laser Welding Process," TRW, \$20,000 (first phase), 5/02-4/03. (PI: H. L. Tsai)
- 9) "Modeling of Hybrid Laser-Arc Welding," GM R&D Center, \$30,000 (first phase), 5/02-12/02. (PI: H. L. Tsai)

VII. Report of Inventions

None